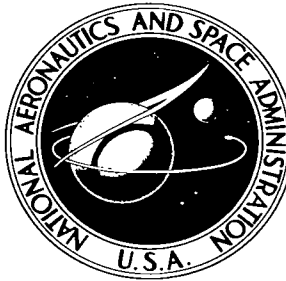
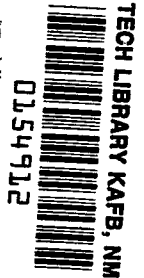


NASA TECHNICAL NOTE



NASA TN D-2394

LOAN COPY: RETU
AFWL (WLIL-2
KIRTLAND AFB, N



NASA TN D-2394

MEASUREMENTS OF HUMAN TRANSFER FUNCTION WITH VARIOUS MODEL FORMS

by James J. Adams and Hugh P. Bergeron
Langley Research Center
Langley Station, Hampton, Va.



MEASUREMENTS OF HUMAN TRANSFER FUNCTION
WITH VARIOUS MODEL FORMS

By James J. Adams and Hugh P. Bergeron

Langley Research Center
Langley Station, Hampton, Va.

NATIONAL AERONAUTICS AND SPACE ADMINISTRATION

For sale by the Office of Technical Services, Department of Commerce,
Washington, D.C. 20230 -- Price \$1.00

MEASUREMENTS OF HUMAN TRANSFER FUNCTION

WITH VARIOUS MODEL FORMS

By James J. Adams and Hugh P. Bergeron
Langley Research Center

SUMMARY

Human transfer functions, relating the pilot's visual input (i.e., the displayed error) to his stick controller output, have been measured by using an automatic model matching technique. In this method, several gains in an analog model with a fixed, preselected form are automatically adjusted to provide the best match to the time history of the pilot's output. In the present investigation input and output data recorded on magnetic tape were analyzed several times with different model forms to determine whether one form had an advantage over another. The different forms included various amounts of fixed time delay and various arrangements of the gains in the linear portion of the model. Time histories of the outputs, closed-loop characteristics calculated by using the measured transfer functions, and system errors obtained with the model in the loop were examined. Results showed no particular advantage for any one model over all the others. The close agreement in results obtained with several of the models indicates that a good linear model for a human pilot has been obtained. Results also indicate that use of this model gives smaller system errors than use of a pilot.

INTRODUCTION

In references 1 and 2 transfer functions of human pilots operating in a fixed-base, single-axis control loop were determined for various controlled element dynamics. The method used was a model matching technique in which the form of the model was preselected and three gains included in the model were automatically adjusted to provide the best possible match to the pilot's output. The form used in these tests was kept as simple as possible yet consistent with the type of control function expected. The present investigation was carried out to determine whether a more elaborate model would give a better match or more significant results.

In the present investigation model forms that included a time delay were tried. Also, the linear portion of the model was altered to include four variables instead of three. This modification involved changing the denominator, or lag terms, of the model. Closed-loop characteristics for the complete system, pilot plus controlled element dynamics, were calculated and were compared with the results presented in reference 2. The human pilot was replaced by the

model pilot in the control loop, and the resulting time history of the system error was compared with that obtained with the human pilot. All tests were conducted by using data stored on magnetic tape; therefore, it was possible to make direct comparisons in all cases.

SYMBOLS

A	model feedback gain representative of lag breakpoint frequency, or damping factor, radians/sec
B	model feedback gain representative of lag breakpoint frequency, radians/sec, or ω_n^2 , radians ² /sec ²
K	adjustment loop gain
K_1, K_2	particular model gains
K_3	time delay, sec
s	Laplace operator, sec ⁻¹
x	difference between pilot output and analog pilot output
α	general gain
δ	model output, volts
$\delta', \delta'', \delta'''$	output of analog pilot at intermediate points, volts
ϵ	displayed error (system error), volts
ζ	damping ratio
ω	frequency, radians/sec
ω_n	undamped natural frequency, radians/sec

A dot over a symbol indicates a derivative with respect to time.

APPARATUS

A block diagram of the control loop in which the pilot operated and a model gain adjustment loop is shown in figure 1. The control loop consisted of an oscilloscope display, a lightweight spring-restrained center-located control stick, and the analog simulation of dynamics. A disturbance signal was entered between the output of the dynamics and the display. This disturbance was obtained from a Gaussian noise generator with two first-order filters with break

frequencies of 1 radian per second. The task was presented as a compensatory tracking task in which the pilot was required to keep the moving indicator aligned with a fixed reference mark. The simulated dynamics included four systems which varied from an easy-to-handle rate mechanism $2/s$ to a more difficult acceleration system $10/s^2$ and included a third-order system with an oscillatory factor $\frac{10}{s(s^2 + 3s + 10)}$ which is typical of good airplane pitch characteristics. The numerators of these dynamics were adjusted so that reasonable control-stick deflections were required in each test. The particular tests used in the present investigation are the third-day tests of pilot E presented in reference 2.

The method used to adjust the linear gains in the model matched to the pilot is fully described in references 1 and 2. In this method the rate of change of the gain to be adjusted is given by the expression

$$\dot{\alpha} = Kx \frac{\partial x}{\partial \alpha} \quad (1)$$

where

x difference between pilot output and model output

α gain to be adjusted

The partial derivatives used in each case are given in the appendix. These derivatives are indicated by the box labeled "Filter" in the block diagram of figure 1. A separate gain adjustment loop was provided for each gain in the model, and all gains were adjusted simultaneously.

The time delay, or transport delay, incorporated in the model was generated by a passive delay line. With this device it was possible to set the delay at fixed values up to 0.2 second. Sample delays of step inputs (fig. 2) show that the device had an adequate frequency response for the present tests. Since the device changed the amplitude of the signal, the gain of the input signal was always adjusted to provide the proper amplitude for the output in the tests.

The time delay was used in conjunction with the linear model used in reference 2; then the complete analytical expression for the model is

$$\frac{\text{Model output}}{\text{Input}} = \frac{K_1 A + K_1 K_2 s}{(A + s)^2} e^{-K_3 s} \quad (2)$$

In these tests the time delay K_3 was set at 0, 0.1, 0.15, and 0.2 second, and the linear gains K_1 , K_2 , and A were automatically adjusted to provide the best match between the model and the pilot.

Two other forms for the linear portion of the model were also tried. In the second form the two first-order lags included in the model were allowed to vary independently. The complete model form in this case is

$$\frac{\text{Model output}}{\text{Input}} = \frac{K_1 B + K_1 K_2 s}{(A + s)(B + s)} e^{-K_3 s} \quad (3)$$

A third form investigated put the denominator in the form of an unfactored quadratic; thus,

$$\frac{\text{Model output}}{\text{Input}} = \frac{K_1 + K_1 K_2 s}{s^2 + As + B} e^{-K_3 s} \quad (4)$$

The third form is a general form that contains the first two forms. This form allows the model to assume an oscillatory character; the first two forms could not do so.

These various model forms are similar to those used in references 3 to 8. In the present investigation, by means of data stored on magnetic tape, all models were used with the same input to provide a critical examination which would display any advantage that one model may have over the others.

RESULTS AND DISCUSSION

Figure 3 shows a sample time history of a test run showing the displayed error, the pilot's control output, the output of the model, and the gain adjustment; the model form used was $\frac{K_1 B + K_1 K_2 s}{(A + s)(B + s)}$. The gain adjustment shown in figure 3 can be compared with that for the same test shown in reference 2 and repeated here in figure 4 using the form $\frac{K_1 A + K_1 K_2 s}{(A + s)^2}$. The time histories of

K_1 and K_2 (fig. 3) contain a high-frequency variation that was not present in the analysis shown in reference 2. This effect is probably due in part to the use of higher adjustment loop gains (K in eq. (1)) than those used in reference 2. Higher gains in all the adjustment loops were used in an attempt to achieve a faster adjustment of the A and B gains, but, even so, the adjustment of A and B was slower than that achieved with the corresponding gain τ in reference 2. This slower response was also noted with the quadratic model form.

The effect of time delays of 0, 0.1, 0.15, and 0.2 second on the match of time histories of the model to the pilot is shown in figure 5. It can be seen that there is no noticeable improvement in the match with any of the delay values. Measurements of the root-mean-square values of the difference between the pilot and the model show, in general, a slight decrease with increase in delay up to 0.15 second, but show a noticeable increase with further increase in delay up to 0.2 second. Therefore, the value of 0.15 second was selected for all further presentation of data in which the time delay was included.

The effect of change in model form, with and without a time delay of 0.15 second, is shown in figures 6 to 8. The individual figures are for three

controlled element dynamics, $2/s$, $\frac{10}{s(s+1)}$, and $10/s^2$. The data for the $10/s^2$ dynamics are repeated in figure 9 with an expanded time scale to show the detail of the tests better. A close examination of these time histories reveals short periods of time when one form appears to provide a better match than another; however, the advantage is not consistent with any one form. Measurements of the root mean square of the difference between the pilot and model did not indicate any advantage.

Different values of the gains were measured with the different model forms. Measured values for all dynamics tested are given in table I. To illustrate the effect of adding a time delay of 0.15 second to the model form $\frac{K_1 A + K_1 K_2 s}{(A + s)^2}$, open-loop frequency-response plots for the model pilot with three different dynamics are presented in figures 10 to 12. These figures show that the changes in the linear parts of the model that occur when the time delay is added are such as to keep the response at lower frequencies the same in both amplitude ratio and phase angle even though differences occur at higher frequencies. The decrease in phase angle brought about by the increase in A compensates for the increase in phase angle added by the time delay.

To determine further whether different values of gains occurring with different model forms had any real significance, two tests were applied. The closed-loop characteristics of the complete systems were calculated. Also the models were inserted in the loop in place of the pilot and, by using the same disturbance time history used with the pilot in each case, the time history of the system error and the root-mean-square value for the system error were determined. Closed-loop characteristics including the model with a time delay were calculated by using a linear approximation for the delay. This approximation consists of the first two terms of a Padé expansion and is written

$$-\frac{\left(s - \frac{2}{K_3}\right)}{\left(s + \frac{2}{K_3}\right)}$$

The closed-loop characteristics and root-mean-square values are listed in table I. The data show a very marked similarity for all the dynamics in the closed-loop frequency, damping ratio, real roots, and root-mean-square value of the error with the model forms $\frac{K_1 A + K_1 K_2 s}{(A + s)^2}$, $\frac{K_1 B + K_1 K_2 s}{(A + s)(B + s)}$, and

$\frac{K_1 s + K_1 K_2 s}{(A + s)(B + s)} e^{-0.15s}$. Other model forms show instances in which the data are not in good agreement with data mentioned previously. With the quadratic form, a much larger change in damping ratio with a change in dynamics was obtained. Lower damping ratios, even negative damping in one case ($10/s^2$), were obtained with the form $\frac{K_1 A + K_1 K_2 s}{(A + s)^2} e^{-0.15s}$ and with the quadratic form with time delay.

There is no basis for determining which form results in correct closed-loop characteristics. Since three of the forms agree closely in results, it is concluded that these results are the closest to being correct. Since the form $\frac{K_1 A + K_1 K_2 s}{(A + s)^2}$ gives a match to the pilot which is as good as any other form, it is the preferred one because it requires the least amount of equipment to mechanize.

The root-mean-square values of the system error obtained with the pilot in the loop and with the analog model in the loop are listed in table I and may be compared. A typical value for the root mean square of the disturbance in all these cases was 2.7 volts. Sample time histories with the model form

$\frac{K_1 A + K_1 K_2 s}{(A + s)^2}$ in the loop and with the pilot in the loop are presented in figures 13 to 15.

These data indicate that much better control is obtained with the model in the loop than with the pilot in the loop. Both time histories and root-mean-square values show that the best agreement in the error is obtained for dynamics of 2/s. In tests with higher order dynamics there are instances in the time histories where an abrupt disturbance occurs and the error obtained with the model and with the pilot are very similar both in time variation and in the amplitude of the error. The instance at the 2-minute point in figure 14 is a good example. When the disturbance is more gentle, larger errors occur with the pilot controlling than occur with the model controlling. These tests illustrate that that part of the pilot's output that does not correlate with a linear model is not useful in reducing the root mean square of the error.

The particular case for $10/s^2$ dynamics chosen for the present investigation was unusual in two respects. The control motions contained a higher frequency than usual, and the closed-loop characteristics were better than usual in that both frequency and damping ratio were high. In fact, the frequency and damping ratio were both higher than that obtained with the $\frac{10}{s(s + 1)}$ dynamics; this result is contrary to the trend shown in all data presented in reference 2. Putting this particular model, with gains $K_1 = 4$, $A = 9.5$, $K_2 = 8$, in the loop with dynamics of $10/s^2$ resulted in a smaller root-mean-square value of the error than was obtained with the model for the $\frac{10}{s(s + 1)}$ dynamics although the root-mean-square value with the pilot in the loop with $10/s^2$ dynamics was higher than that with the pilot in the loop with $\frac{10}{s(s + 1)}$ dynamics. The use of a more typical set of model gains, $K_1 = 3$, $A = 7$, $K_2 = 6.5$ (also taken from ref. 2), restored the expected trend in root-mean-square values with change in dynamics. However, the root-mean-square error with the model in the loop was still smaller than that obtained with the pilot. These data are also shown in table I and in figure 15. It is interesting to note the small change in gains required to bring about a fairly large change in the closed-loop system error.

CONCLUDING REMARKS

The transfer functions of a human pilot have been measured by an automatic model matching technique using six different model forms. The time histories of the pilot's output were matched with the same degree of precision for all models. Close agreement among three of the models was achieved in the calculated closed-loop characteristics and in the system error obtained with the model in the loop. This agreement indicates that a good matching linear transfer function for a pilot has been found.

Langley Research Center,
National Aeronautics and Space Administration,
Langley Station, Hampton, Va., April 24, 1964.

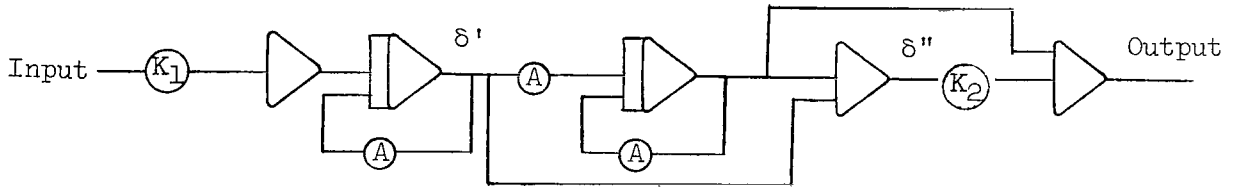
APPENDIX

PARTIAL DERIVATIVES USED IN THE GAIN ADJUSTMENT LOOP FILTERS

The partial derivatives used in the gain adjustment loop filters with each of the models are given in this appendix. For the model with

$$\frac{\text{Output}}{\text{Input}} = \frac{K_1 A + K_1 K_2 s}{(A + s)^2}$$

the model diagram is



and the partial derivatives are

$$\frac{\partial x}{\partial K_1} = \left[\frac{A + K_2 s}{(A + s)^2} \right] (\text{Input})$$

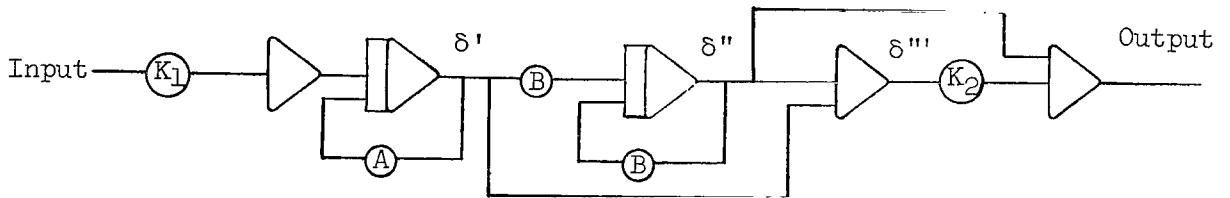
$$\frac{\partial x}{\partial A} = - \left[\frac{A + (2K_2 - 1)s}{(A + s)^2} \right] \delta'$$

$$\frac{\partial x}{\partial K_2} = -\delta''$$

For the model with

$$\frac{\text{Output}}{\text{Input}} = \frac{K_1 B + K_1 K_2 s}{(A + s)(B + s)}$$

the model diagram is



and the partial derivatives are

$$\frac{\partial x}{\partial K_1} = \left[\frac{K_1 B + K_1 K_2 s}{(A + s)(B + s)} \right] (\text{Input})$$

$$\frac{\partial x}{\partial A} = \left[\frac{B + K_2 s}{(A + s)(B + s)} \right] \delta'$$

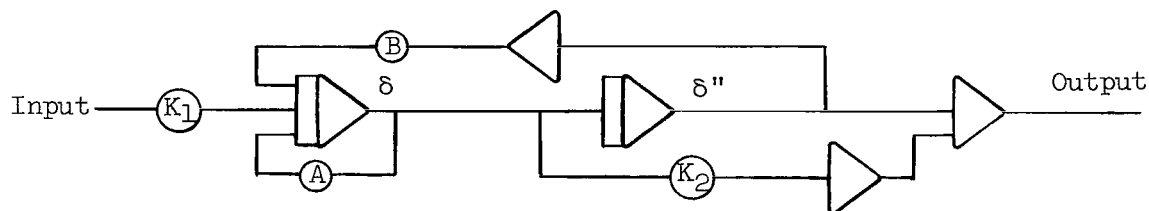
$$\frac{\partial x}{\partial B} = \left[\frac{(K_2 - 1)s}{B(B + s)} \right] \delta''$$

$$\frac{\partial x}{\partial K_2} = -\delta'''$$

For the model with

$$\frac{\text{Output}}{\text{Input}} = \frac{K_1 + K_1 K_2 s}{s^2 + As + B}$$

the analog diagram is



and the partial derivatives are

$$\frac{\partial x}{\partial K_1} = - \left[\frac{1 + K_2 s}{s^2 + As + B} \right] (\text{Input})$$

$$\frac{\partial x}{\partial A} = - \left[\frac{1 + K_2 s}{s^2 + As + B} \right] \delta'$$

$$\frac{\partial x}{\partial B} = \left[\frac{1 + K_2 s}{s^2 + As + B} \right] \delta''$$

$$\frac{\partial x}{\partial K_2} = \delta'$$

REFERENCES

1. Adams, James J.: A Simplified Method for Measuring Human Transfer Functions. NASA TN D-1782, 1963.
2. Adams, James J., and Bergeron, Hugh P.: Measured Variation in the Transfer Function of a Human Pilot in Single-Axis Tasks. NASA TN D-1952, 1963.
3. Elkind, Jerome I.: Characteristics of Simple Manual Control Systems. Tech. Rep. No. 111, Lincoln Lab., M.I.T., Apr. 6, 1956.
4. Hall, Ian A. M.: Effects of Controlled Element on the Human Pilot. WADC Tech. Rep. 57-509 (ASTIA Doc. No. AD 130979), U.S. Air Force, Aug. 1958.
5. Seckel, Edward, Hall, Ian A. M., McRuer, Duane T., and Weir, David H.: Human Pilot Dynamic Response in Flight and Simulator. WADC Tech. Rep. 57-520, ASTIA Doc. No. AD 130988, U.S. Air Force, Aug. 1958.
6. McRuer, Duane T., and Krendel, Ezra S.: The Human Operator as a Servo System Element. Jour. Franklin Inst. Part I, vol. 267, no. 5, May 1959, pp. 381-403. Part II, vol. 267, no. 6, June 1959, pp. 511-536.
7. Ornstein, George N.: Applications of a Technique for the Automatic Analog Determination of Human Response Equation Parameters. Rep. No. NA61H-1, North American Aviation, Inc., Jan. 2, 1961.
8. Kuehnel, Helmut A.: Human Pilots' Dynamic-Response Characteristics Measured in Flight and on a Nonmoving Simulator. NASA TN D-1229, 1962.

TABLE I.- SUMMARY OF DATA WITH VARIOUS CONTROLLED ELEMENT DYNAMICS

(a) 2/s dynamics

Analog pilot form	Measured gains				Closed-loop characteristics			Root-mean-square error, volts, with -	
	K ₁	A	B	K ₂	Oscillatory		Real roots	Pilot	Analog pilot
					ω _n , radians/sec	ζ			
$\frac{K_1 A + K_1 K_2 s}{(A + s)^2}$	4	3		2	4.36	0.54	-1.26	0.86	0.89
$\frac{K_1 A + K_1 K_2 s}{(A + s)^2} e^{-0.15s}$	7	10		3.5	8.14	.57	-1.24; -22.7		
$\frac{K_1 B + K_1 K_2 s}{(A + s)(B + s)}$	1	1	7	7	3.7	.93	-1.0	.86	.83
$\frac{K_1 B + K_1 K_2 s}{(A + s)(B + s)} e^{-0.15s}$	9	5.5	9	2	5.2	.41	-4.1; -19.5	.86	.67
$\frac{K_1 + K_1 K_2 s}{s^2 + As + B}$	3	25	0	16			-5.0; -6.4; -18.5	.86	.67
$\frac{K_1 + K_1 K_2 s}{s^2 + As + B} e^{-0.15s}$	3	25	0	16	6.3	.48	-6.4; -32.2	.86	.46

TABLE I.- SUMMARY OF DATA WITH VARIOUS CONTROLLED ELEMENT DYNAMICS - Continued

(b) $\frac{10}{s(s + 2.5)}$ dynamics

Analog pilot form	Measured gains				Closed-loop characteristics			Root-mean-square error, volts, with -	
					Oscillatory		Real roots		
	K ₁	A	B	K ₂	ω _n , radians/sec	ξ		Pilot	Analog pilot
$\frac{K_1 A + K_1 K_2 s}{(A + s)^2}$	3	5		2	2.8	0.40	-2.5; -7.8	1.2	0.95
$\frac{K_1 A + K_1 K_2 s}{(A + s)^2} e^{-0.15s}$	5.5	7		4	3.8 14.8	.12 .93	-1.6	1.2	.96
$\frac{K_1 B + K_1 K_2 s}{(A + s)(B + s)}$	7	8	7	2	3.3	.39	-4.0; -11.0	1.2	.80
$\frac{K_1 B + K_1 K_2 s}{(A + s)(B + s)} e^{-0.15s}$	8	11	12	4	3.46 17.9	.35 .38	-3.35	1.2	.93
$\frac{K_1 + K_1 K_2 s}{s^2 + As + B}$	40	60	40	1.5	3.1	.37	-0.68; -59.5	1.2	.83
$\frac{K_1 + K_1 K_2 s}{s^2 + As + B} e^{-0.15s}$	100	34	110	.5	3.7	.16	-1.9; -18.4; -28.3	1.2	.86

TABLE I.- SUMMARY OF DATA WITH VARIOUS CONTROLLED ELEMENT DYNAMICS - Continued

(c) $\frac{10}{s(s+1)}$ dynamics

Analog pilot form	Measured gains				Closed-loop characteristics			Root-mean-square error, volts, with -	
	K_1	A	B	K_2	Oscillatory		Real roots	Pilot	Analog pilot
					ω_n , radians/sec	ζ			
$\frac{K_1 A + K_1 K_2 s}{(A + s)^2}$	2.5	6.5		5.5	3.45	0.37	-1.24; -10.1	1.6	0.86
$\frac{K_1 A + K_1 K_2 s}{(A + s)^2} e^{-0.15s}$	5	11		9	4.1 18.4	.18 .91	-1.28	1.6	.89
$\frac{K_1 B + K_1 K_2 s}{(A + s)(B + s)}$	5	10	6	4	3.7	.38	-1.7; -12.4	1.6	.75
$\frac{K_1 B + K_1 K_2 s}{(A + s)(B + s)} e^{-0.15s}$	7	17	16	10	3.7 22.6	.43 .93	-2.09	1.6	.80
$\frac{K_1 + K_1 K_2 s}{s^2 + As + B}$	50	40	80	1	3.6	.27	-1.0; -38.2	1.6	.69
$\frac{K_1 + K_1 K_2 s}{s^2 + As + B} e^{-0.15s}$	70	30	160	1	4.4 22.0	.15 .95	-1.0	1.6	.75

TABLE I.- SUMMARY OF DATA WITH VARIOUS CONTROLLED ELEMENT DYNAMICS - Continued

(d) $\frac{10}{s^2}$ dynamics

Analog pilot form	Measured gains				Closed-loop characteristics			Root-mean-square error, volts, with -	
					Oscillatory		Real roots		
	K ₁	A	B	K ₂	ω _n , radians/sec	ζ		Pilot	Analog pilot
$\frac{K_1 A + K_1 K_2 s}{(A + s)^2}$	4 3	9.5 7		8 6.5	3.9 3.71	0.40 .21	-1.78; -14.1 -1.38; -10.9	2.0 2.2	0.77 1.57
$\frac{K_1 A + K_1 K_2 s}{(A + s)^2} e^{-0.15s}$	4	12		20	5.2 20.4	-.39 .97	-.66	2.0	2.5
$\frac{K_1 B + K_1 K_2 s}{(A + s)(B + s)}$	6.5	15	6	5	3.7	.35	-1.7; -16.7	2.0	.67
$\frac{K_1 B + K_1 K_2 s}{(A + s)(B + s)} e^{-0.15s}$	5	25	10	15	3.7 23.4	.33 .96	-.86	2.0	.73
$\frac{K_1 + K_1 K_2 s}{s^2 + As + B}$	100	35	150	.8	4.5	.27	-1.5; -30.9	2.0	.65
$\frac{K_1 + K_1 K_2 s}{s^2 + As + B} e^{-0.15s}$	90	35	250	1.2	4.5 24	.12 .33	-1.0	2.0	.81

TABLE I.- SUMMARY OF DATA WITH VARIOUS CONTROLLED ELEMENT DYNAMICS - Concluded

(e) $\frac{10}{s(s^2 + 3s + 10)}$ dynamics									
Analog pilot form	Measured gains				Closed-loop characteristics			Root-mean-square error, volts, with -	
					Oscillatory	Real roots			
	K_1	A	B	K_2	ω_n , radians/sec			ζ	Pilot
$\frac{K_1 A + K_1 K_2 s}{(A + s)^2}$	6	7		5	3.2 7.9	0.18 .96	-0.6	1.6	1.2
$\frac{K_1 A + K_1 K_2 s}{(A + s)^2} e^{-0.15s}$	6	7.5		10	5.4 9.3	.85 .86	-0.44; -14.8	1.6	1.5
$\frac{K_1 B + K_1 K_2 s}{(A + s)(B + s)}$	6	7.5	5	6	3.4 7.5	.10 .95	-0.47	1.6	1.0
$\frac{K_1 B + K_1 K_2 s}{(A + s)(B + s)} e^{-0.15s}$	7	10	10	10	3.2 11.4	.11 .85	-0.49; -15.7	1.6	1.1
$\frac{K_1 + K_1 K_2 s}{s^2 + As + B}$	50	25	60	1.5	3.4	.09	-0.42; -4.7 -22.2	1.6	1.0
$\frac{K_1 + K_1 K_2 s}{s^2 + As + B} e^{-0.15s}$	75	15	80	1	3.34 10.4	.03 .76	-0.6; -14.7	1.6	1.3

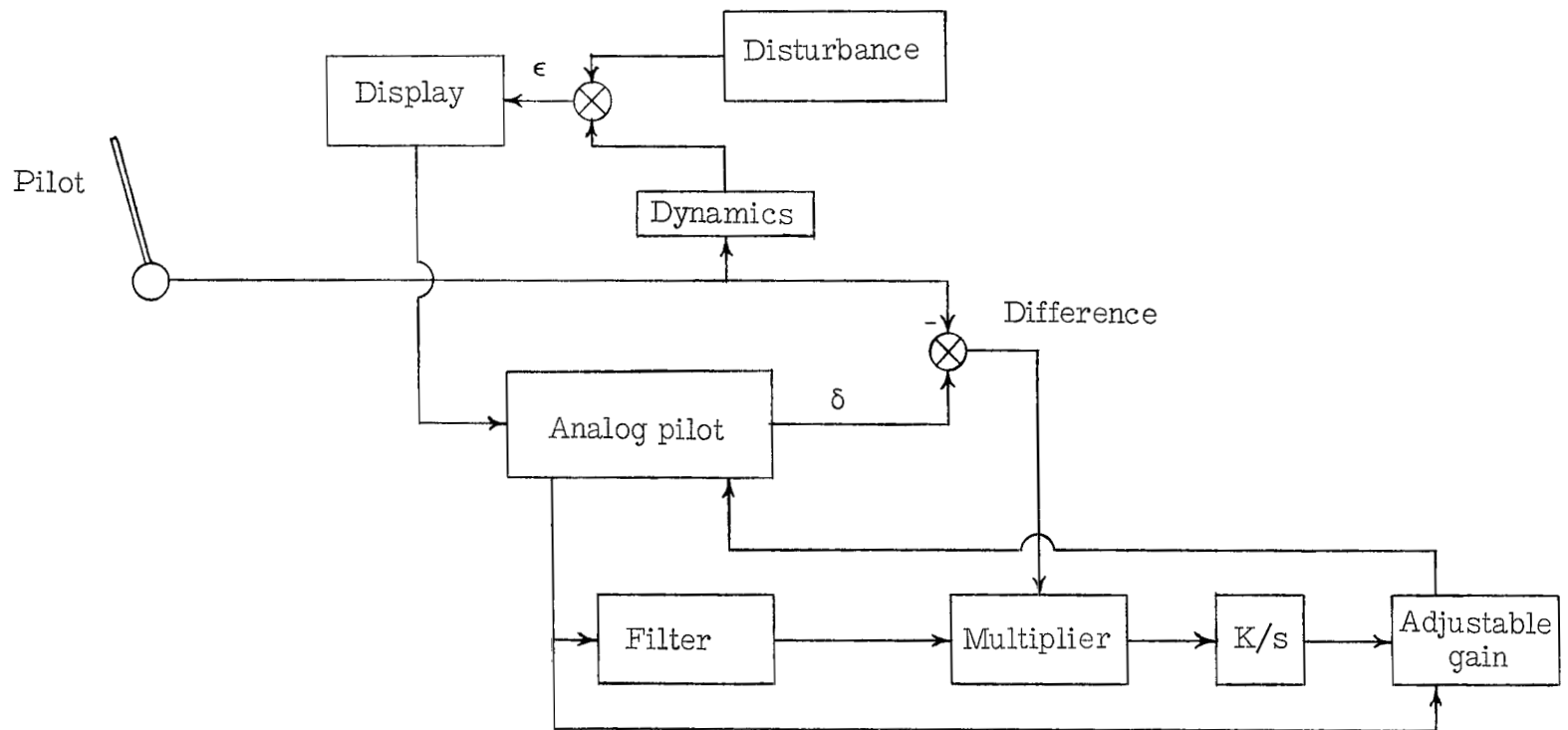
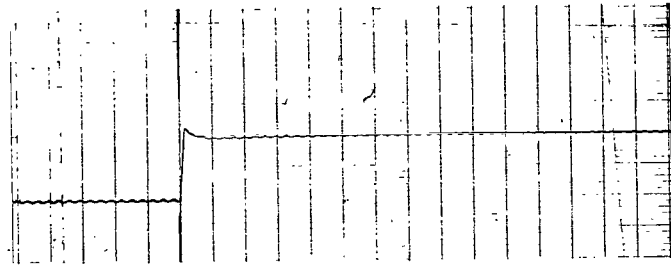


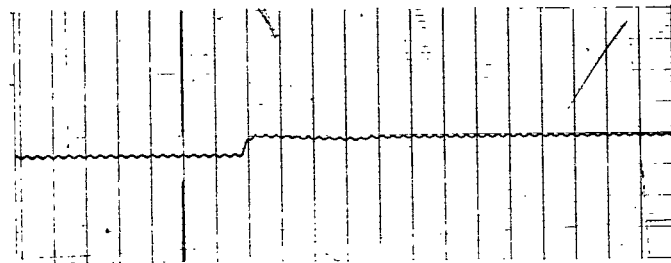
Figure 1.- Block diagram of test equipment.

Time delay,
0.1 sec

Input

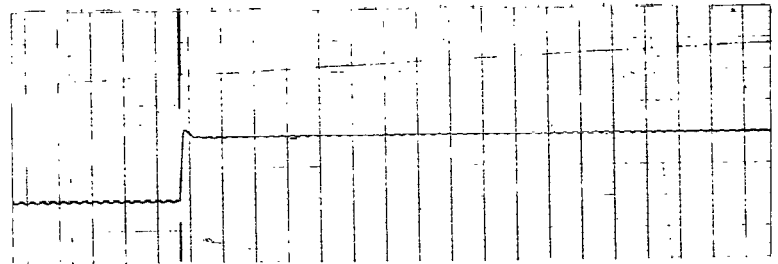


Response



Time delay,
0.2 sec

Input



Response

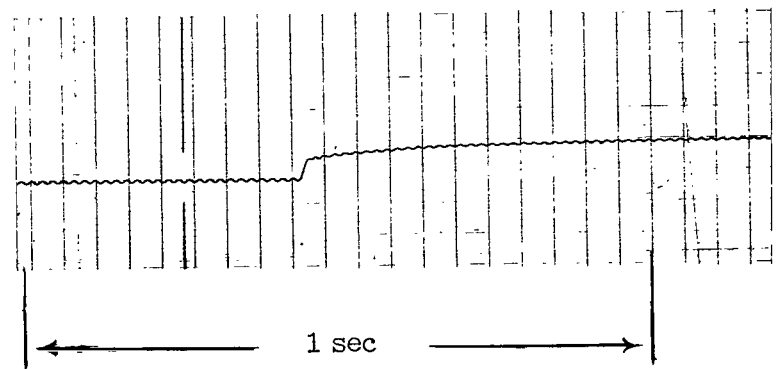


Figure 2.- Time-delay response for step input.

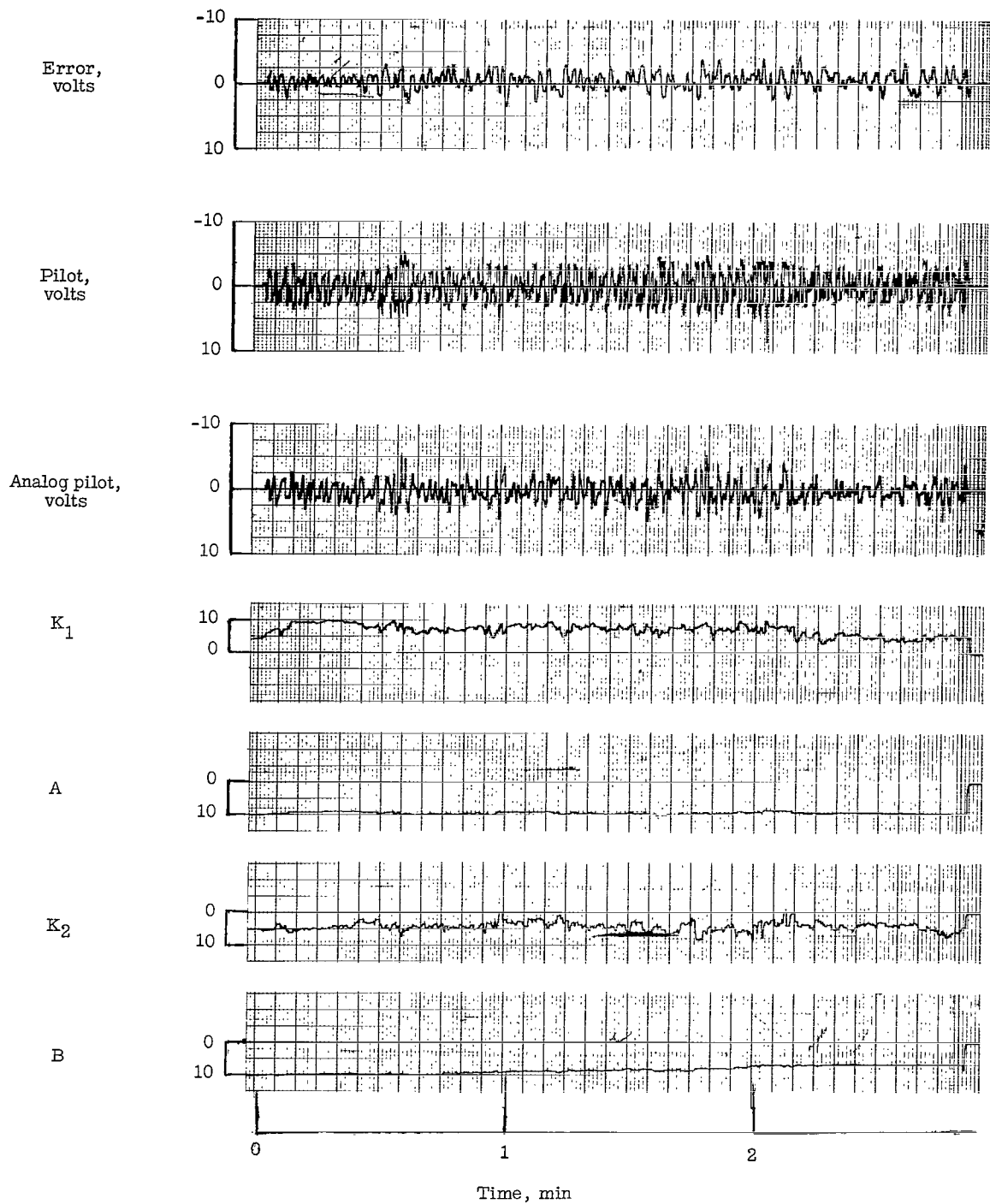


Figure 3.- Sample test with dynamics of $\frac{10}{s(s+1)}$ and model form of $\frac{K_1 B + K_1 K_2 s}{(A+s)(B+s)}$.

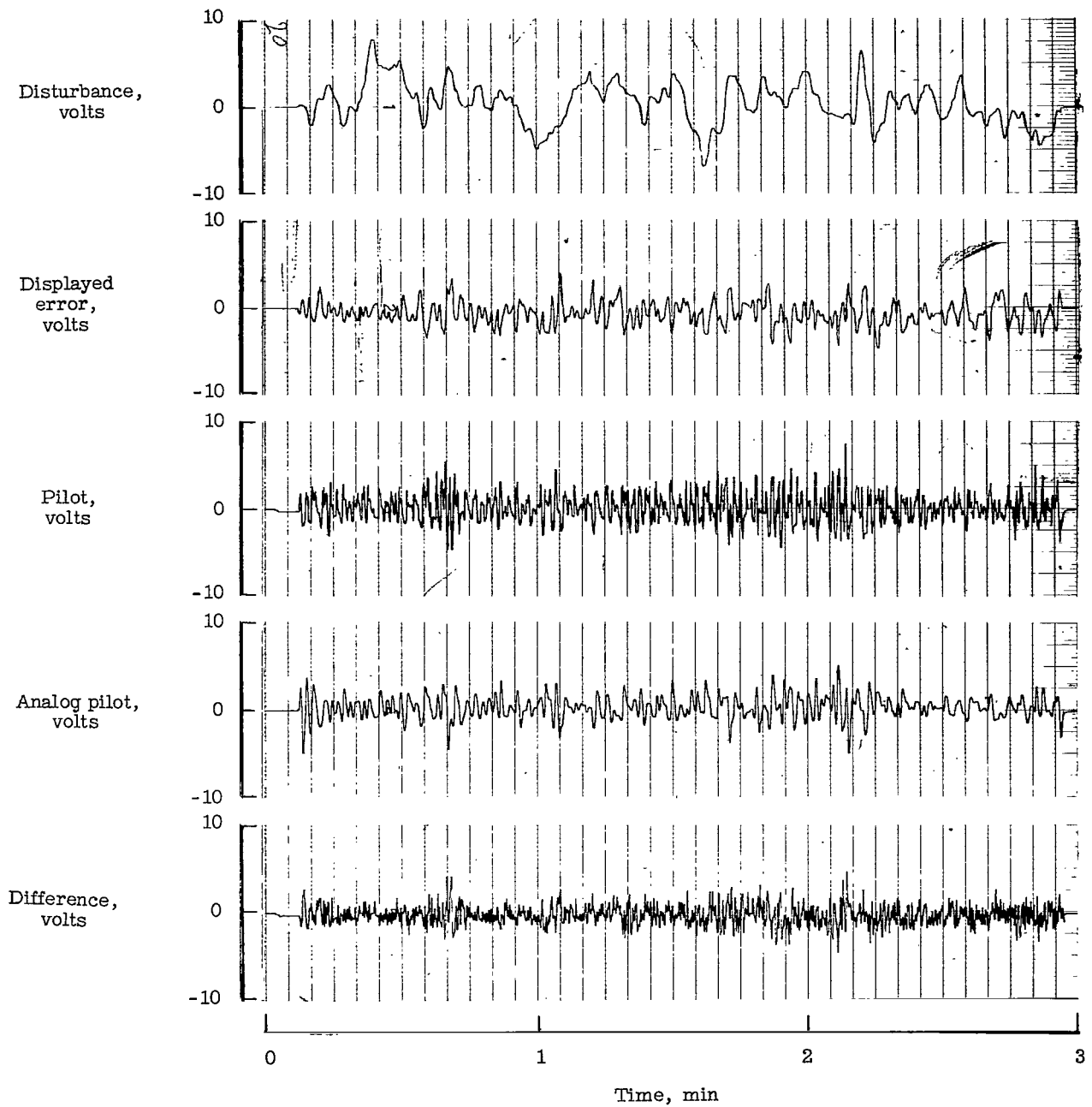


Figure 4.- Sample run with dynamics of $\frac{10}{s(s+1)}$ and model form $\frac{K_1A + K_1K_2s}{(A+s)^2}$.

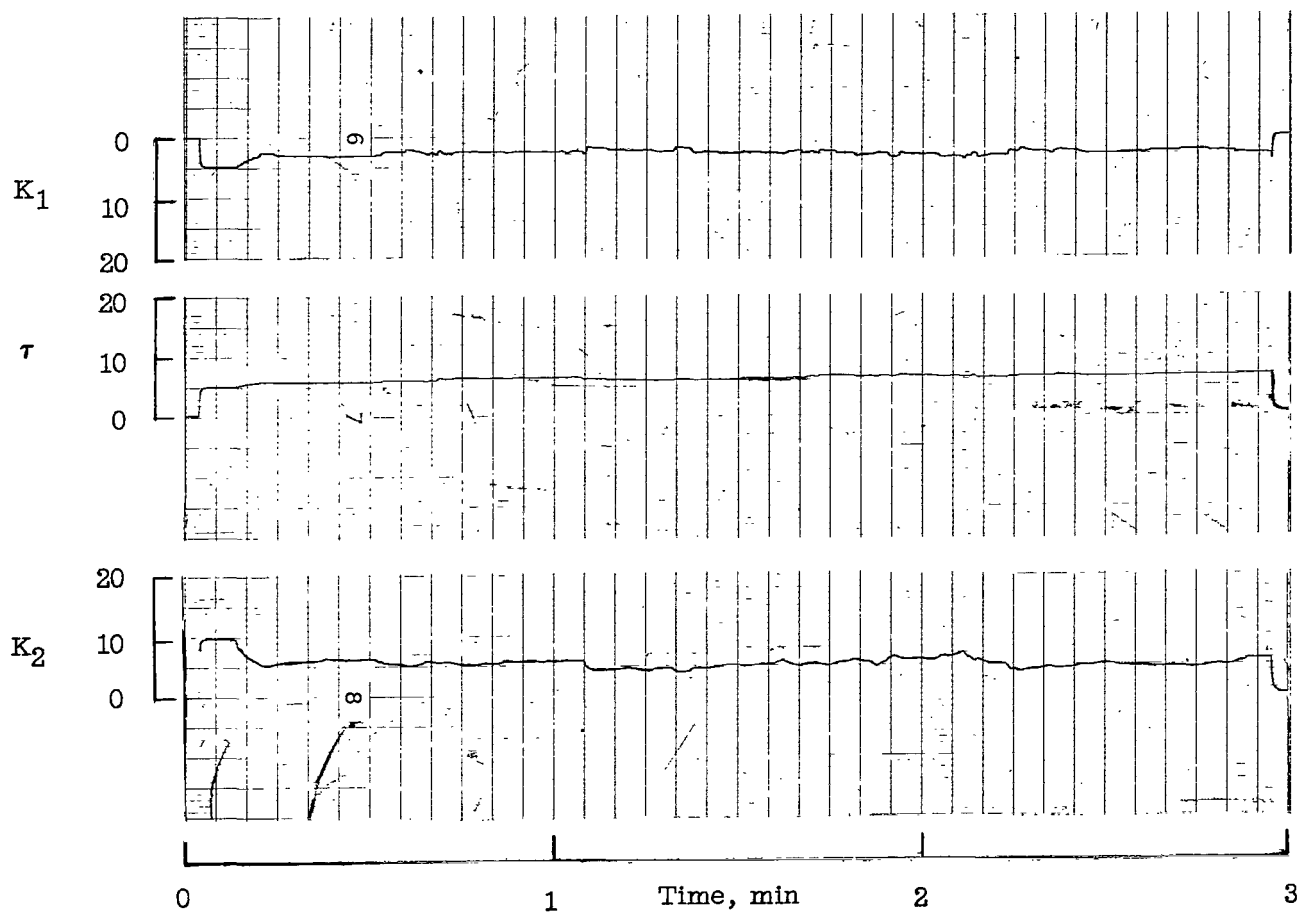


Figure 4.- Concluded.

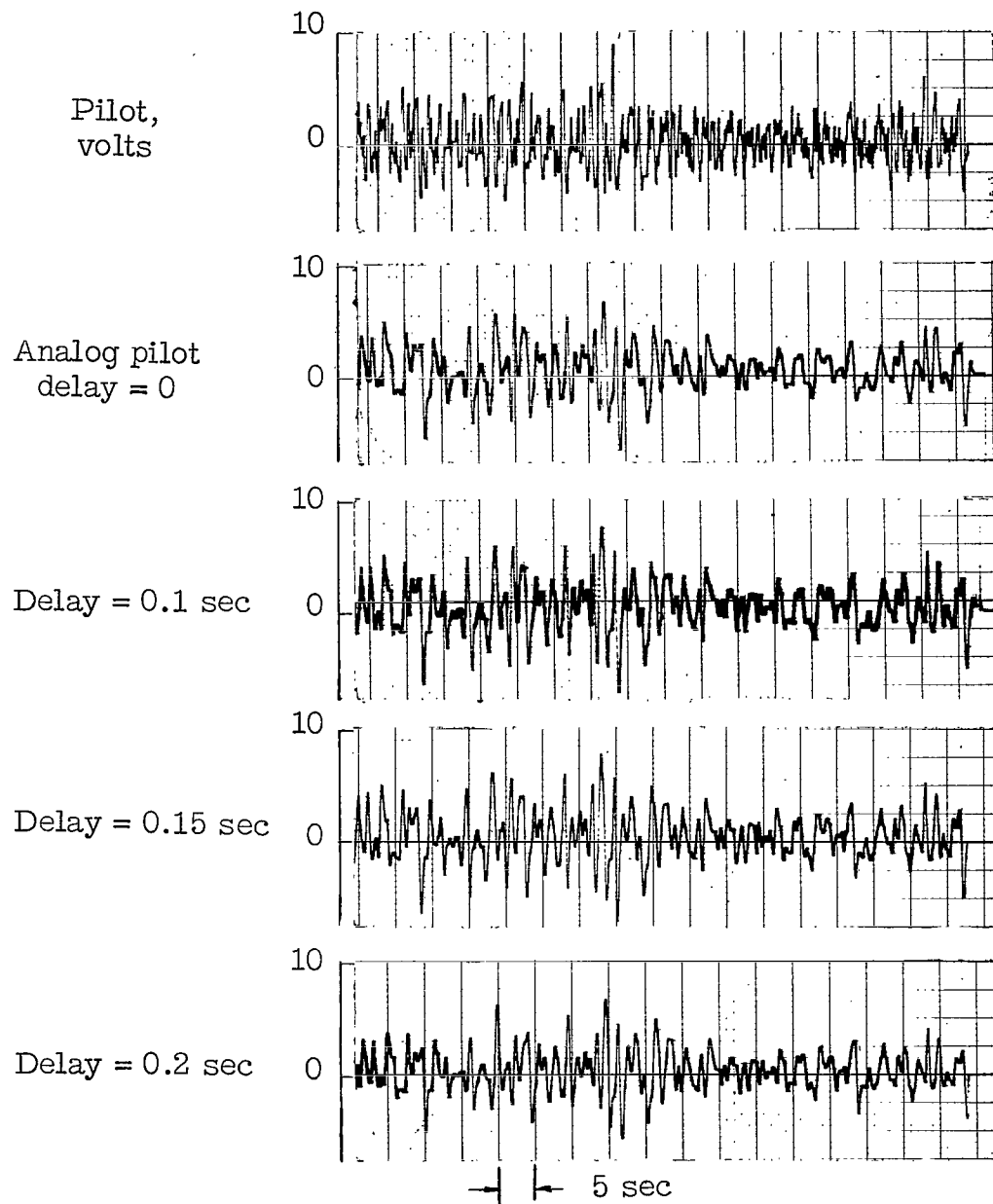


Figure 5.- Time histories illustrating analog pilot match with various time delays with dynamics of $\frac{10}{s(s+1)}$ and model form $\frac{K_1A + K_1K_2s}{(A+s)^2} e^{-K_3s}$.

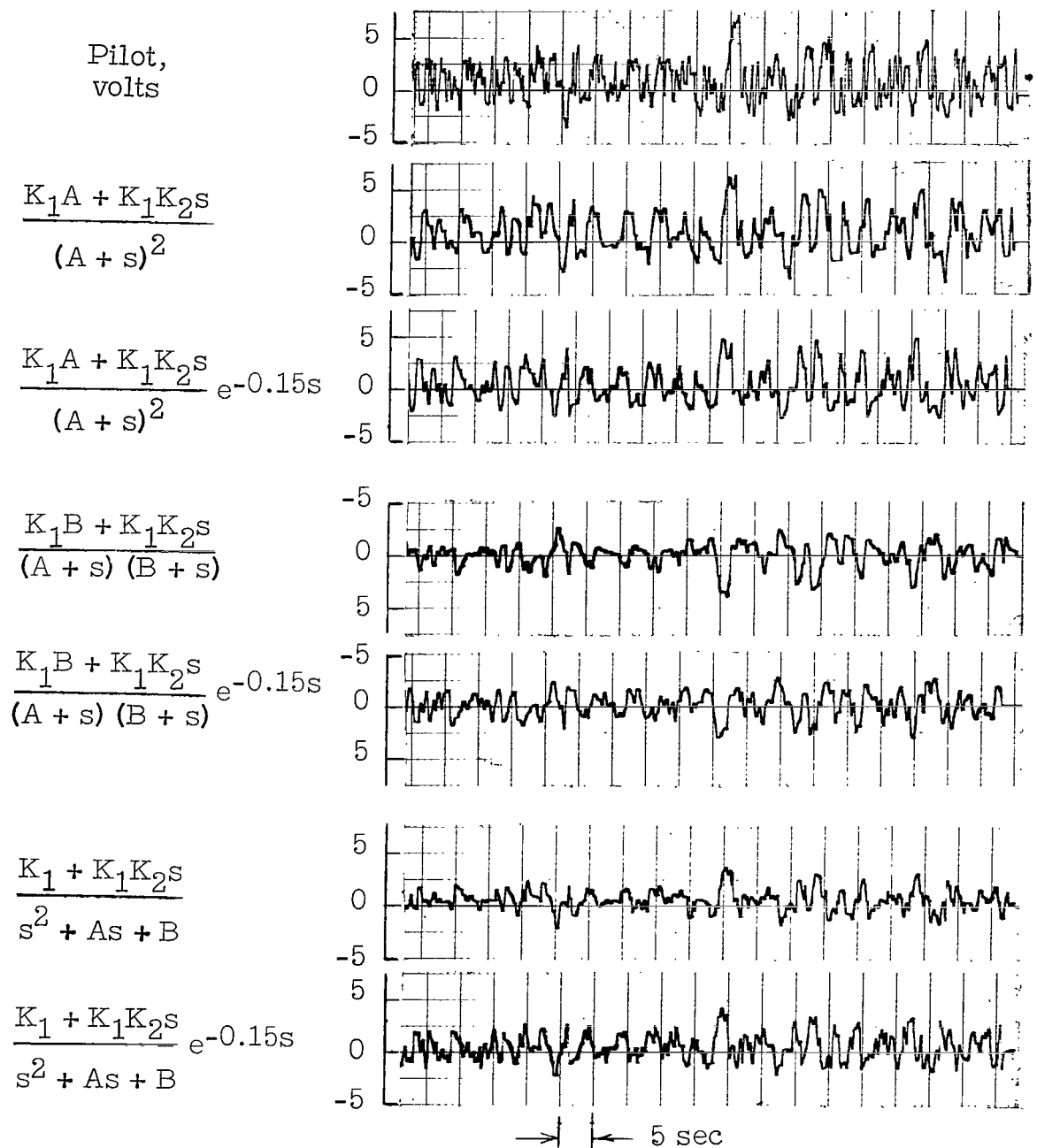


Figure 6.- Time histories illustrating match of different analog pilot forms with $2/s$ dynamics.

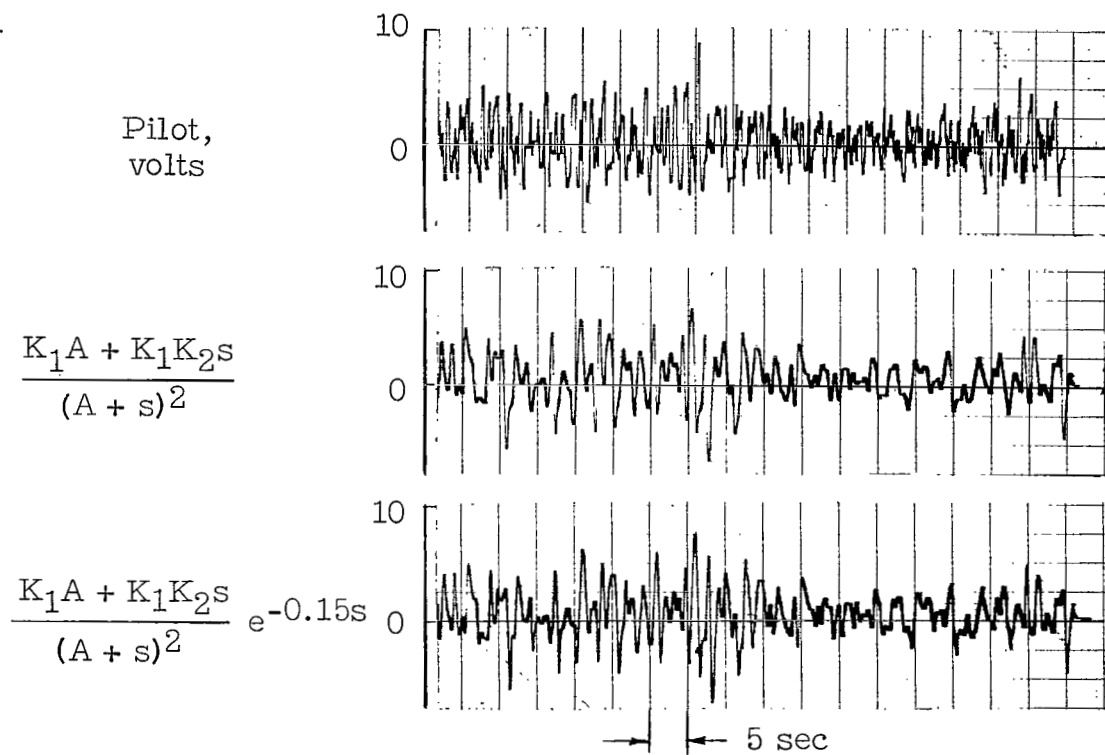
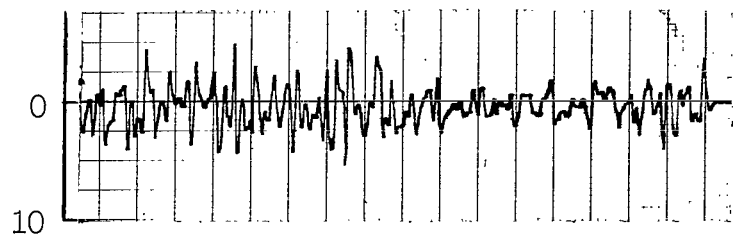
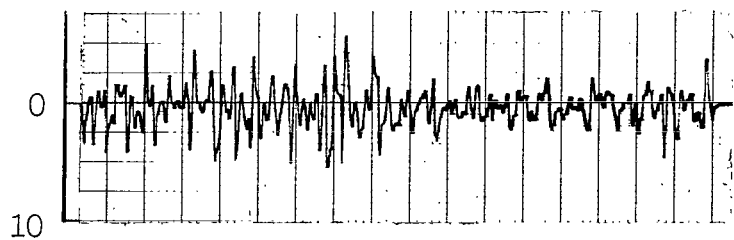


Figure 7.- Time histories illustrating match of different analog pilot forms with $\frac{10}{s(s+1)}$ dynamics.

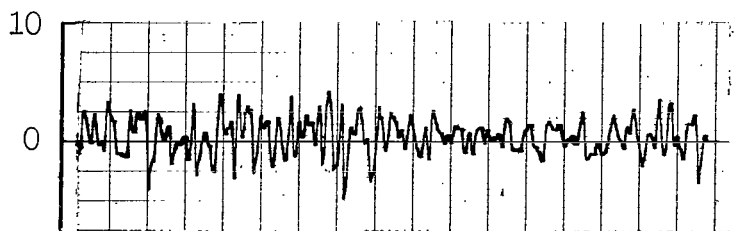
$$\frac{K_1 B + K_1 K_2 s}{(A + s)(B + s)}$$



$$\frac{K_1 B + K_1 K_2 s}{(A + s)(B + s)} e^{-0.15s}$$



$$\frac{K_1 + K_1 K_2 s}{s^2 + As + B}$$



$$\frac{K_1 + K_1 K_2 s}{s^2 + As + B} e^{-0.15s}$$

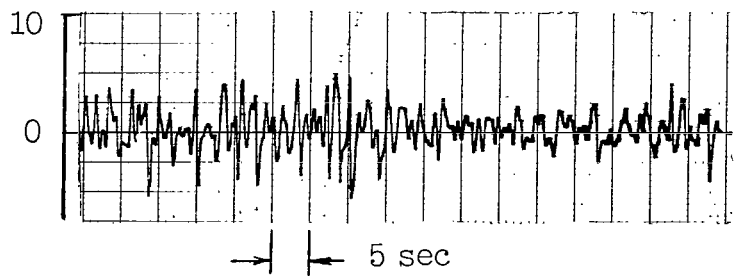
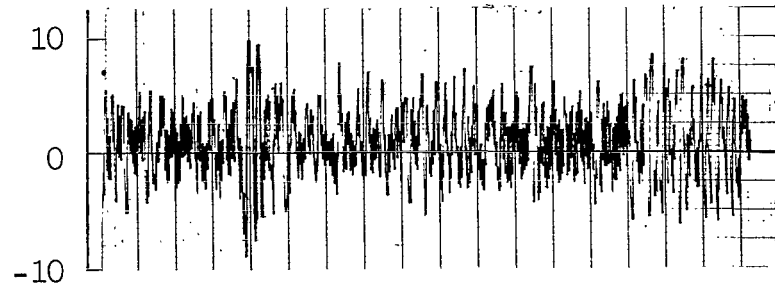
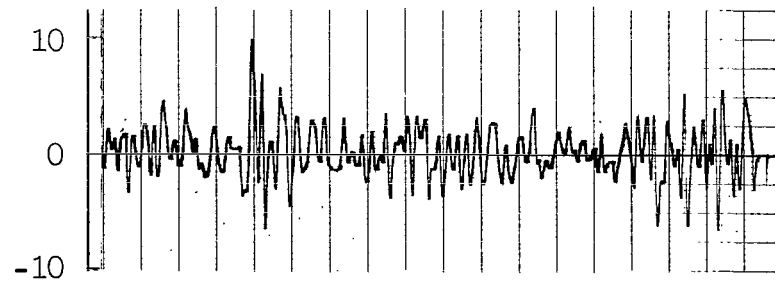


Figure 7.- Concluded.

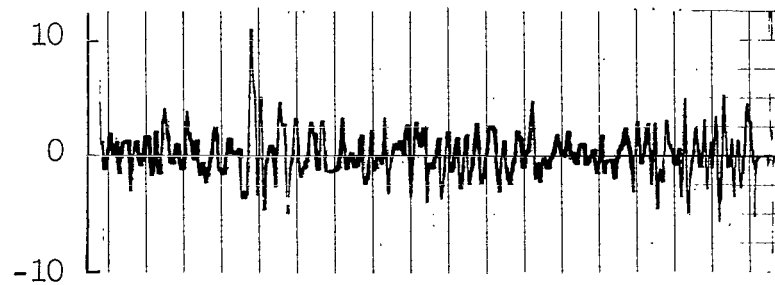
Pilot,
volts



$$\frac{K_1 A + K_1 K_2 s}{(A + s)^2}$$



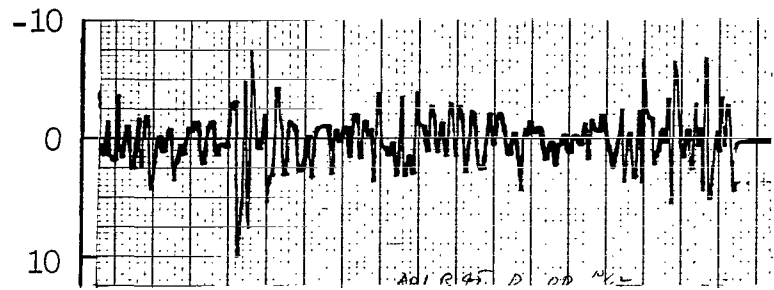
$$\frac{K_1 A + K_1 K_2 s}{(A + s)^2} e^{-0.15s}$$



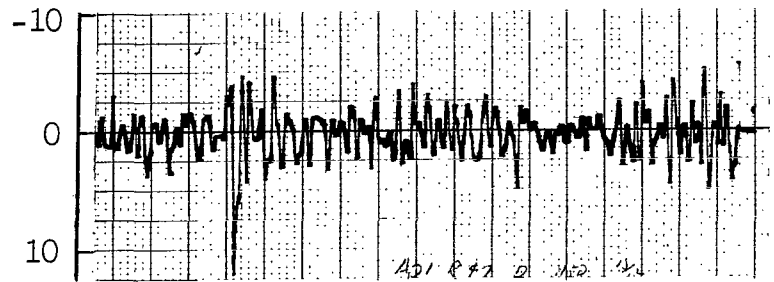
→ | ← 5 sec

Figure 8.- Time history illustrating match with different analog pilot forms with $10/s^2$ dynamics.

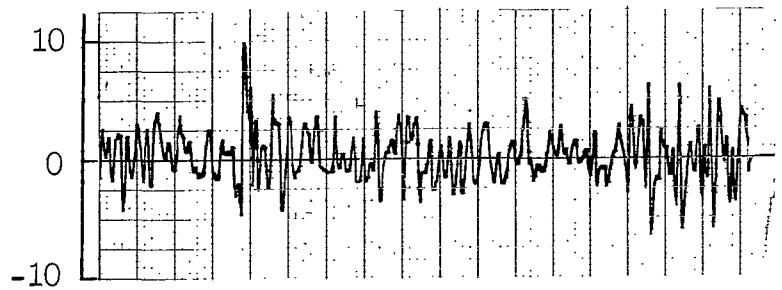
$$\frac{K_1 B + K_1 K_2 s}{(A + s)(B + s)}$$



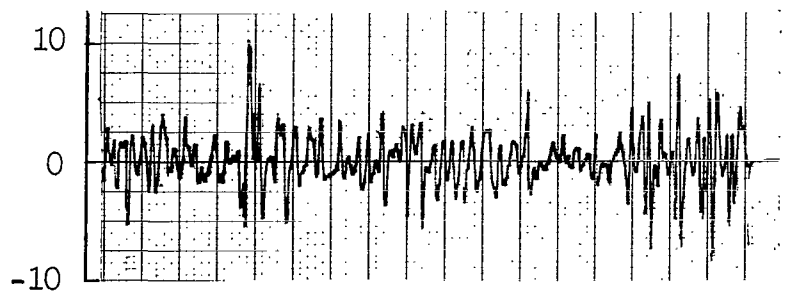
$$\frac{K_1 B + K_1 K_2 s}{(A + s)(B + s)} e^{-0.15s}$$



$$\frac{K_1 + K_1 K_2 s}{s^2 + As + B}$$



$$\frac{K_1 + K_1 K_2 s}{s^2 + As + B} e^{-0.15s}$$



→ | ← 5 sec

Figure 8.- Concluded.

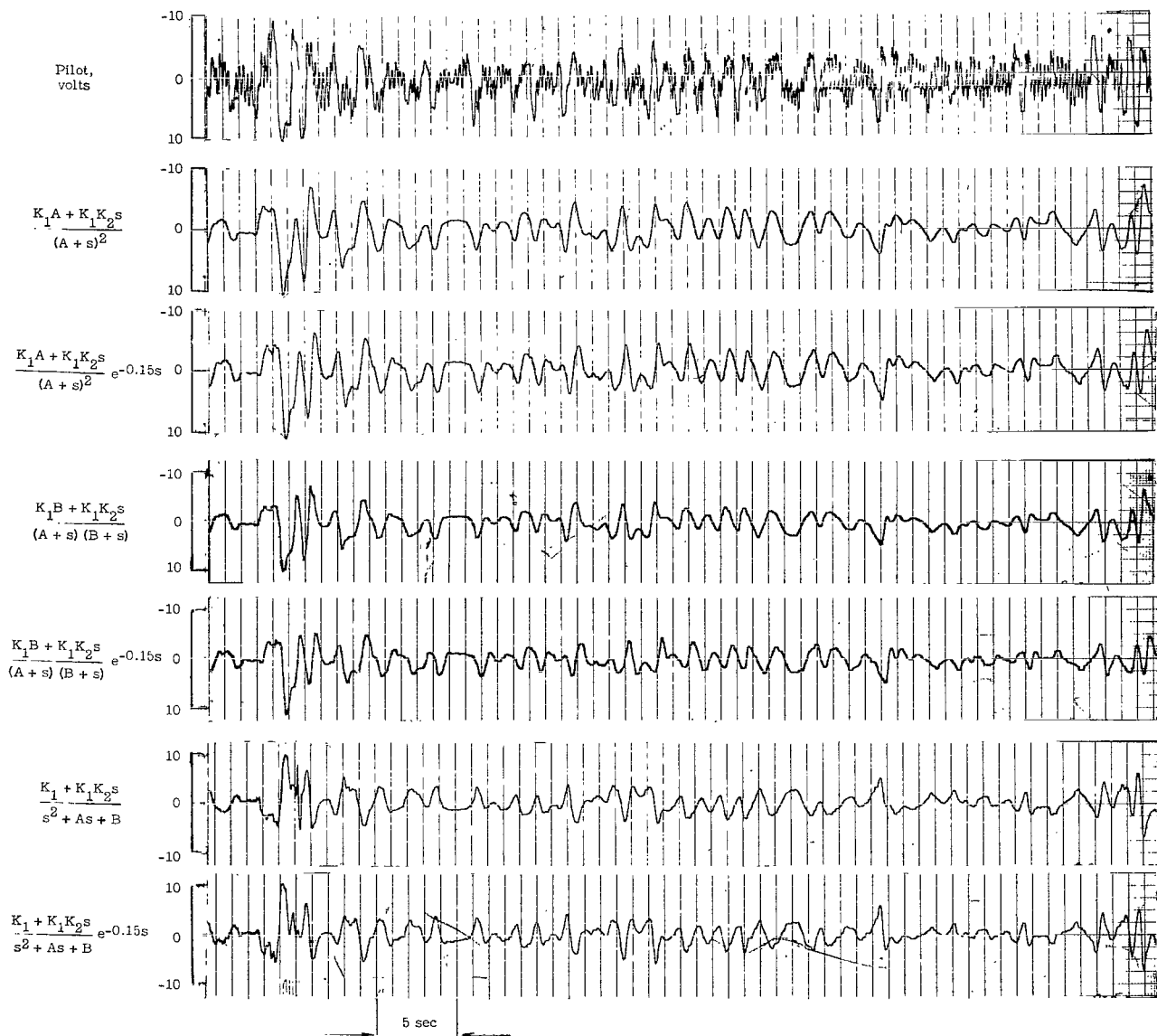


Figure 9.- Time histories illustrating match of different analog pilot forms with $10/s^2$ dynamics.

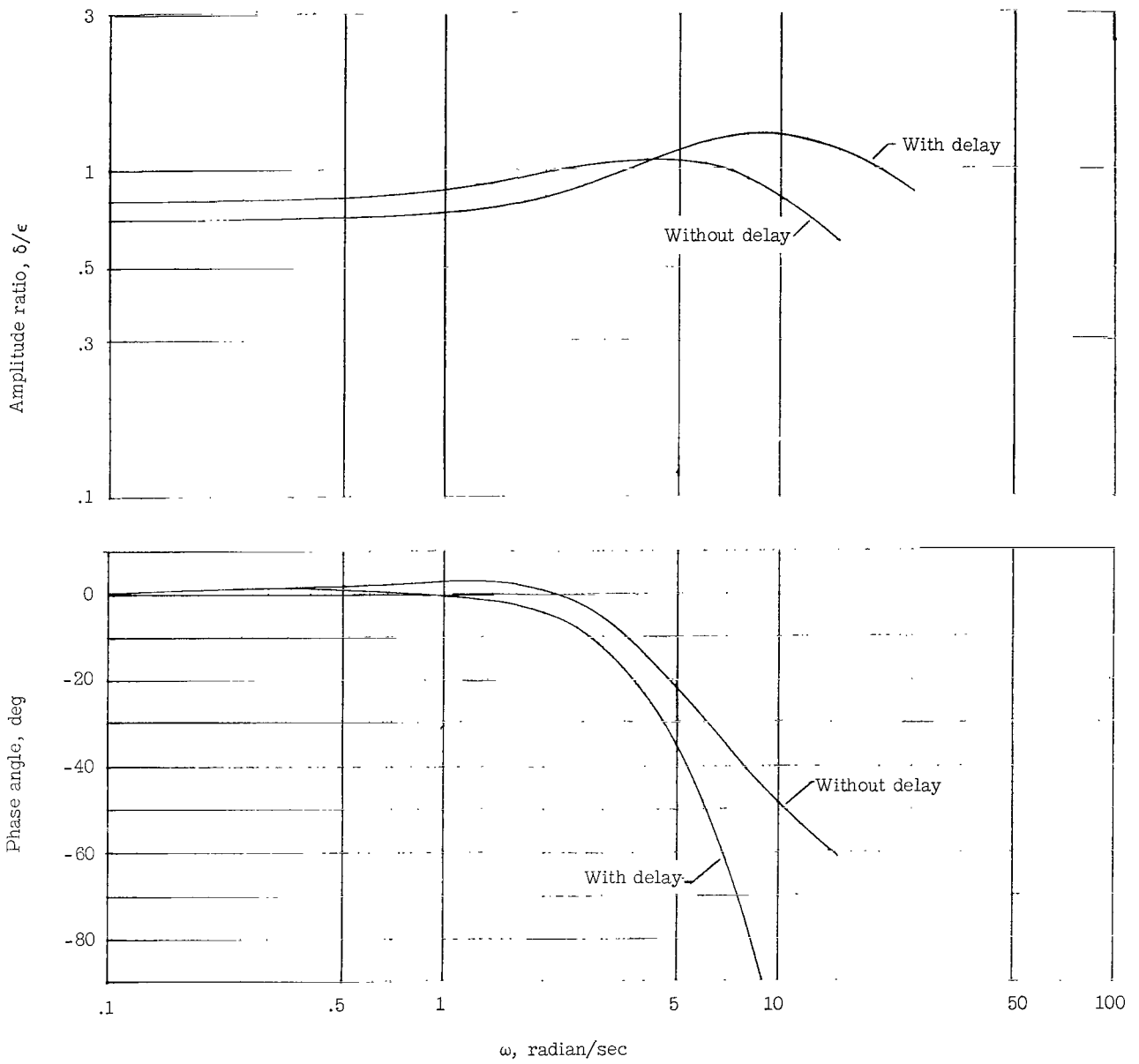


Figure 10.- Model pilot frequency response with dynamics of $2/s$ and model forms of

$$\frac{K_1 A + K_1 K_2 s}{(A + s)^2} \quad \text{and} \quad \frac{K_1 A + K_1 K_2 s}{(A + s)^2} e^{-0.15s}.$$

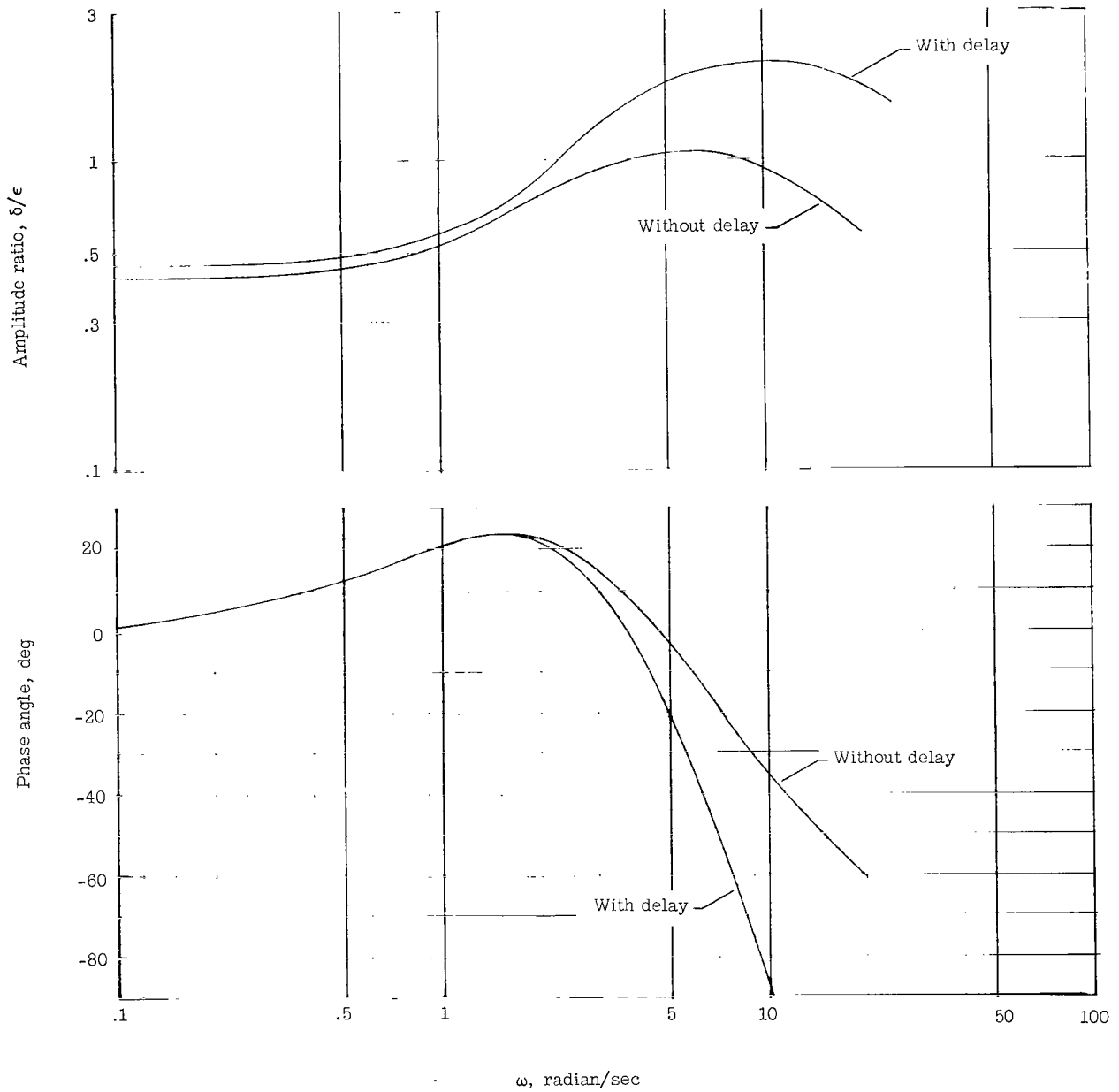


Figure 11.- Model pilot frequency response with dynamics of $\frac{10}{s(s+1)}$ and model forms of

$$\frac{K_1 A + K_1 K_2 s}{(A + s)^2} \quad \text{and} \quad \frac{K_1 A + K_1 K_2 s}{(A + s)^2} e^{-0.15s}.$$

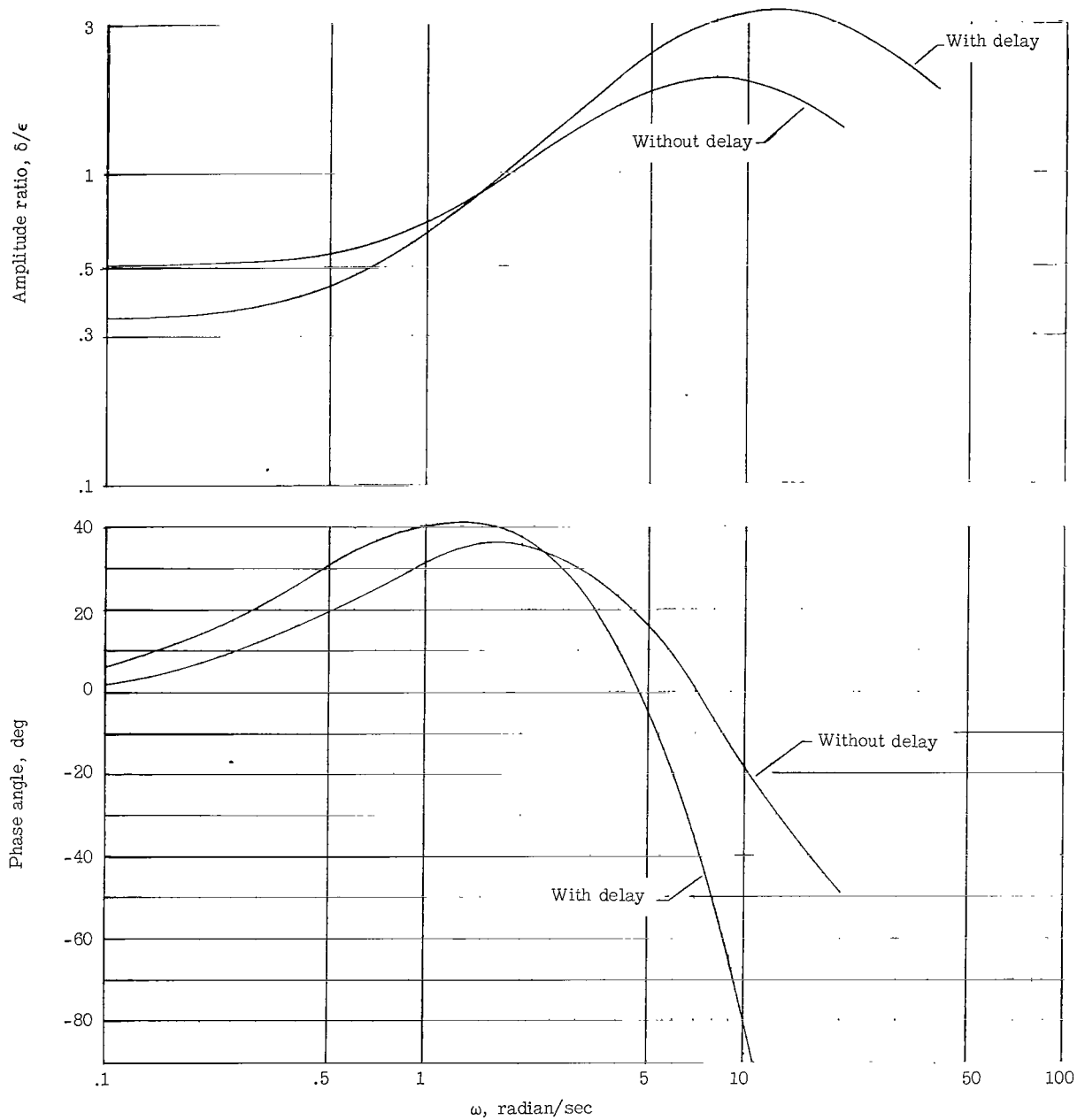


Figure 12.- Model pilot frequency response with dynamics of $10/s^2$ and model forms of

$$\frac{K_1 A + K_1 K_2 s}{(A + s)^2} \quad \text{and} \quad \frac{K_1 A + K_1 K_2 s}{(A + s)^2} e^{-0.15s}.$$

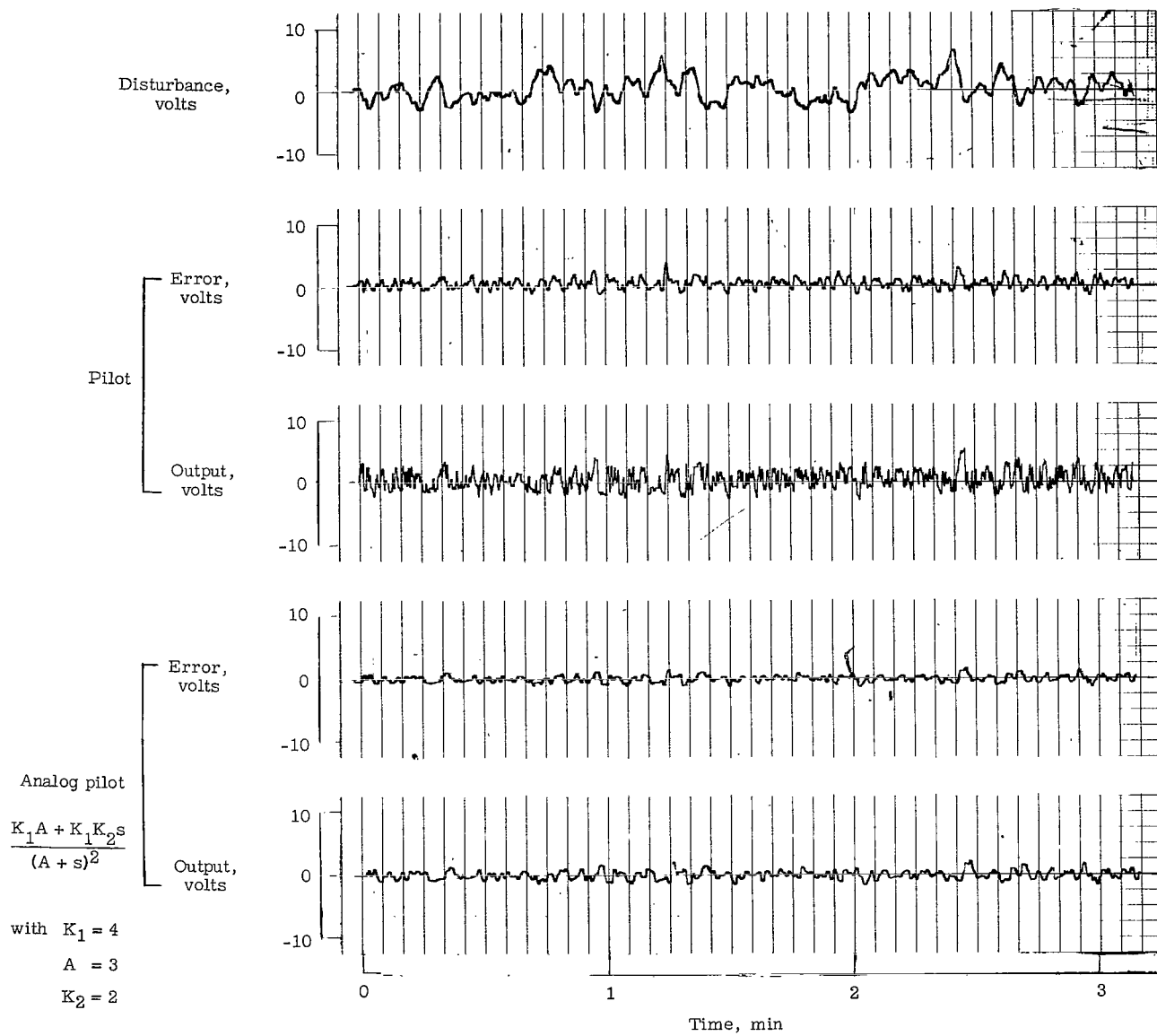


Figure 13.- Comparison of pilot in loop with analog pilot in loop for a dynamics of $2/s$.

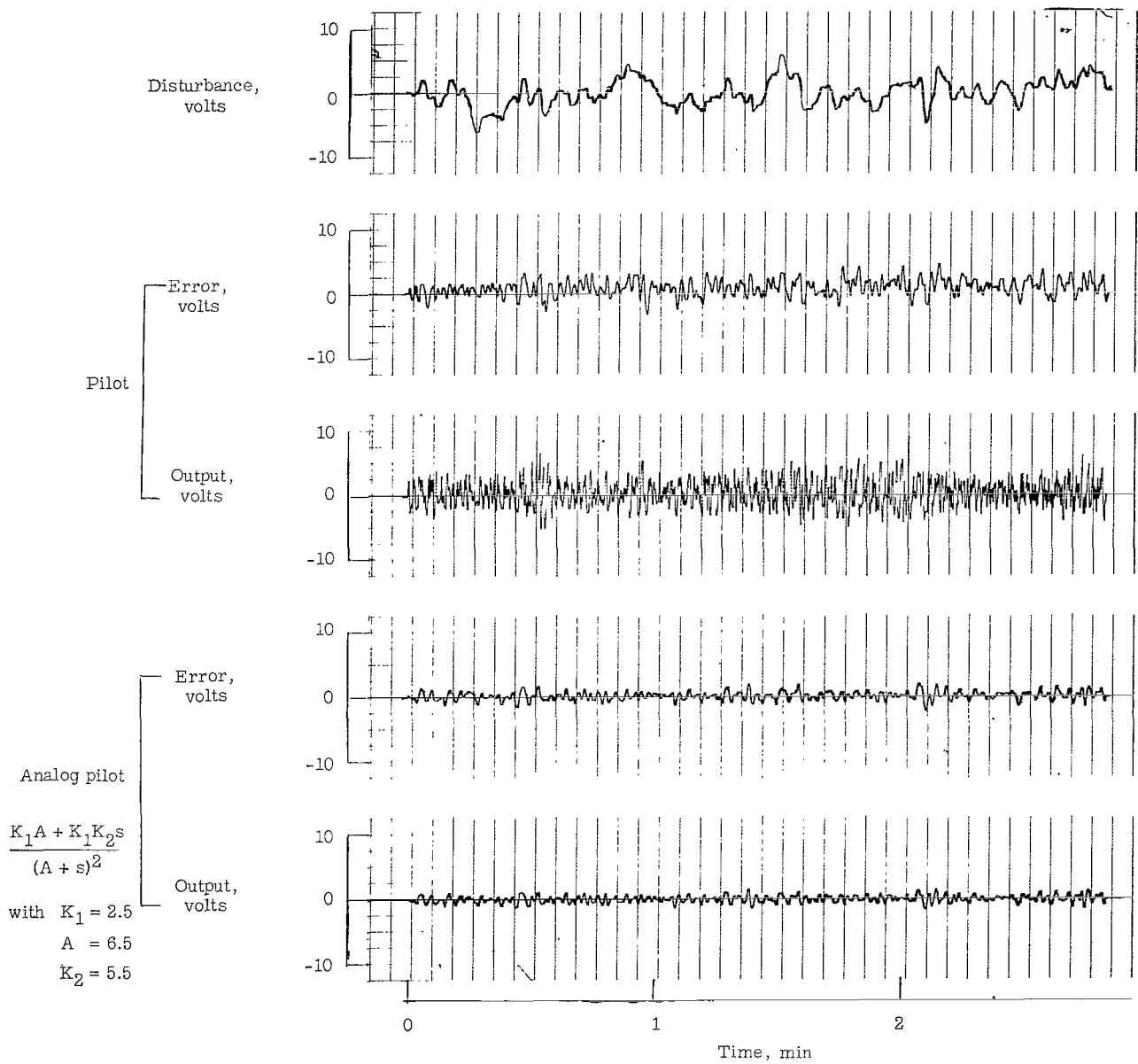


Figure 14.- Comparison of pilot in loop with analog pilot in loop for a dynamics of $\frac{10}{s(s+1)}$.

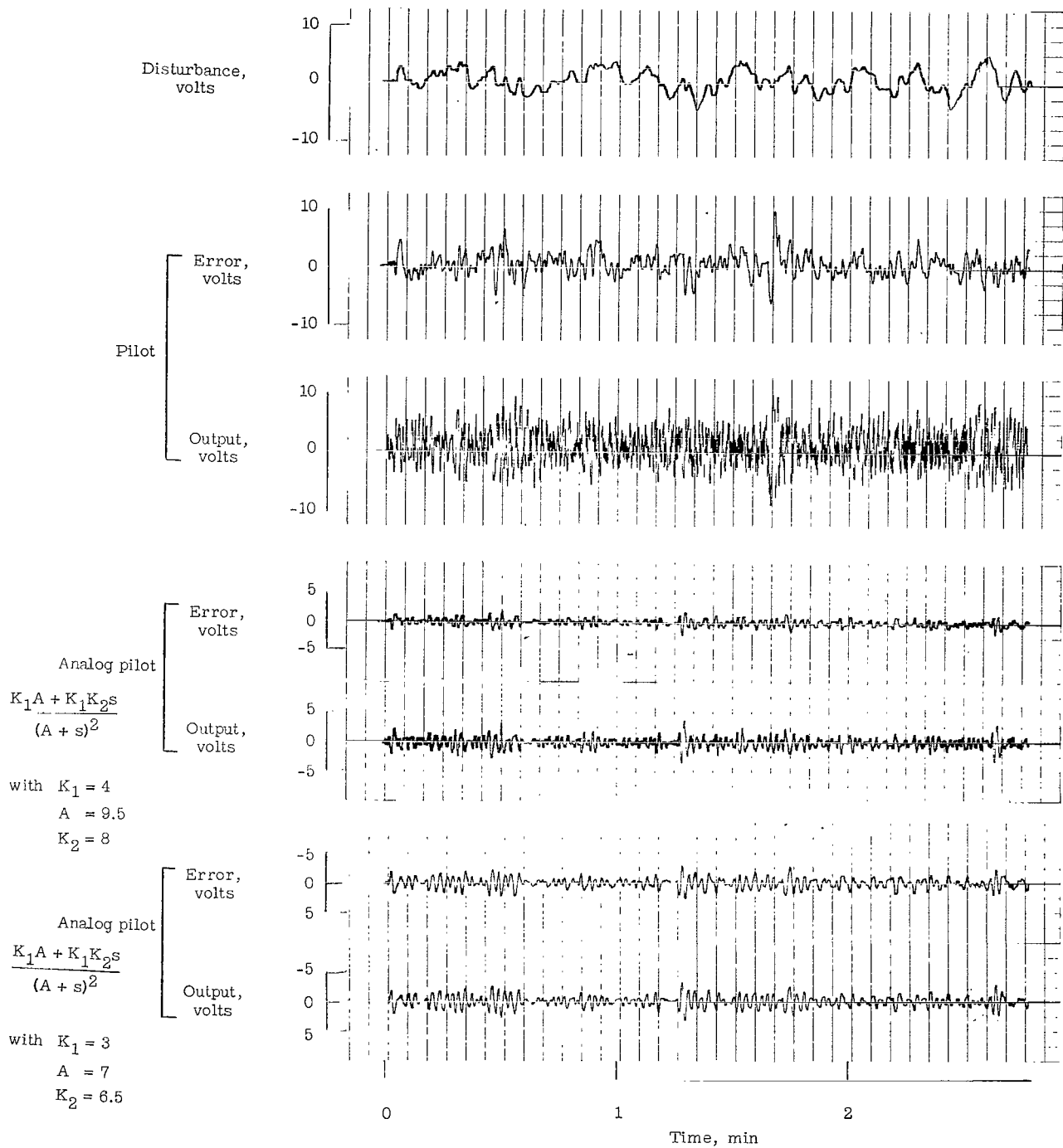


Figure 15.- Comparison of pilot in loop with analog pilot in loop for a dynamics of $10/s^2$.

2.17/85
08

"The aeronautical and space activities of the United States shall be conducted so as to contribute . . . to the expansion of human knowledge of phenomena in the atmosphere and space. The Administration shall provide for the widest practicable and appropriate dissemination of information concerning its activities and the results thereof."

—NATIONAL AERONAUTICS AND SPACE ACT OF 1958

NASA SCIENTIFIC AND TECHNICAL PUBLICATIONS

TECHNICAL REPORTS: Scientific and technical information considered important, complete, and a lasting contribution to existing knowledge.

TECHNICAL NOTES: Information less broad in scope but nevertheless of importance as a contribution to existing knowledge.

TECHNICAL MEMORANDUMS: Information receiving limited distribution because of preliminary data, security classification, or other reasons.

CONTRACTOR REPORTS: Technical information generated in connection with a NASA contract or grant and released under NASA auspices.

TECHNICAL TRANSLATIONS: Information published in a foreign language considered to merit NASA distribution in English.

TECHNICAL REPRINTS: Information derived from NASA activities and initially published in the form of journal articles.

SPECIAL PUBLICATIONS: Information derived from or of value to NASA activities but not necessarily reporting the results of individual NASA-programmed scientific efforts. Publications include conference proceedings, monographs, data compilations, handbooks, sourcebooks, and special bibliographies.

Details on the availability of these publications may be obtained from:

SCIENTIFIC AND TECHNICAL INFORMATION DIVISION
NATIONAL AERONAUTICS AND SPACE ADMINISTRATION
Washington, D.C. 20546